arXiv:1510.00928v1 [cond-mat.stat-mech] 4 Oct 2015

Repulsive Casimir interaction: Boyer oscillators at nanoscale

Jalal Sarabadani,[1,*] Badrosadat Ojaghi Dogahe,[2] and Rudolf Podgornik[3]

[1]*Department of Applied Physics and COMP Center of Excellence, Aalto University School of Science, P.O. Box 11000, FI-00076 Aalto, Espoo, Finland*
[2]*Department of Physics, University of Isfahan, Isfahan 81744, Iran*
[3]*Department of Physics, University of Massachusetts, Amherst, Massachusetts 01003, USA, and Department of Theoretical Physics, J. Stefan Institute, and Department of Physics, Faculty of Mathematics and Physics, University of Ljubljana, SI-1000 Ljubljana, Slovenia*

We study the effect of temperature on the repulsive Casimir interaction between an ideally permeable and an ideally polarizable plate *in vacuo*. At small separations or for low temperatures the quantum fluctuations of the electromagnetic field give the main contribution to the interaction, while at large separations or for high temperatures the interaction is dominated by the classical thermal fluctuations of the field. At intermediate separations or finite temperatures both the quantum and thermal fluctuations contribute. For a system composed of one infinitely permeable plate between two ideal conductors at a finite temperature, we identify a *stable mechanical equilibrium* state, if the infinitely permeable plate is located in the middle of the cavity. For small displacements the restoring force of this *Boyer oscillator* is linear in the deviation from the equilibrium position, with a spring constant that depends inversely on the separation between the two conducting plates and linearly on temperature. Furthermore, an array of such oscillators presents an ideal Einsteinian crystal that displays a fluctuation force between its outer boundaries stemming from the displacement fluctuations of the Boyer oscillators.

A long-range attraction between two ideal flat conductors due to fluctuations of the electromagnetic (EM) field at zero temperature has been discovered by H.B.G. Casimir in 1948 [1] and is directly connected with the change in the quantum vacuum zero-point energy [2]. The magnitude of the Casimir attractive force per unit surface area is, $\frac{F^C}{A} = -\frac{\hbar c \pi^2}{240 H^4}$, where A is the surface area of the plates, $\hbar$ is the Planck constant divided by 2π, c is the speed of light in the vacuum and H is the separation between two plates. In 1955 Lifshitz developed a more general framework to investigate forces between two dispersive dielectric media at finite temperature T [3]. The ensuing *Casimir-Lifshitz interactions* have gained much attention [4–15] as they are one of the direct macroscopic manifestations of the quantum theory. Investigating the Casimir interaction with asymmetric boundary conditions, Boyer in 1974 showed that an infinitely polarizable (ideal conductor) and an infinitely permeable plate (a two-plate Boyer setup) at $T = 0$K repel each other with a repulsive force $F = -(7/8)F^C$ [16]. Later, this result was confirmed by two different methods, the radiation pressure method [17] and the path-integral formalism [18]. Boyer's conclusions are in general consistent with the Lifshitz theory where repulsive Casimir interactions are only possible in asymmetric interaction setups [4], such as a surface with high dielectric response (infinite polarizability of an ideal conductor) apposed to a surface with high magnetic response (infinite permeability) across vacuum [19].

Repulsive Casimir-Lifshitz interactions are well documented also experimentally [20–22]. The Casimir-Lifshitz force between a gold sphere (ϵ_G) and a silica substrate (ϵ_S), when they are immersed in bromobanzene (ϵ_B), has been found to be repulsive ($\epsilon_G > \epsilon_B > \epsilon_S$) [23], just like the force between a permeable yttrium iron garnet (YIG) plate and a ferroelectric $BaTiO_3$ *in vacuo*, possibly implicating the Boyer mechanism in the latter case [24]. The calculated Boyer force per unit area then follows as $\sim 1.3\times10^{-4}$N/m^2 if the plates are separated by 1μm, becoming significantly larger at sub-micron scales. Casimir-Lifshitz interactions are particularly strong on the nanoscale [5] and must therefore be taken into account when designing micro- and nano-electromechanical systems (MEMS and NEMS) [25, 26].

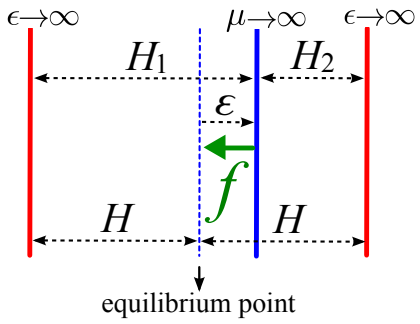

FIG. 1: Schematic depiction of the Boyer oscillator. Two parallel flat ideal conductors ($\epsilon \to \infty$) apposed at separation $2H$, with a parallel flat ideally permeable ($\mu \to \infty$) plate between them. When the permeable plate is moved to the right for ε, which means that $H_1 = H + \varepsilon$ and $H_2 = H - \varepsilon$, the Casimir force F acts on the permeable plate to bring it back to its equilibrium point.

*Electronic address: jalal.sarabadani@aalto.fi

In order to unravel additional details of the repulsive Casimir-Lifshitz interaction we analyze a Boyer setup composed of two ideally polarizable ($\epsilon \to \infty$) plates with an ideally permeable ($\mu \to \infty$) plate in the middle, see Fig. 1, at separation H and temperature T. We explore the possibility of stable equilibria and construct a mechanical oscillator that furthermore leads to an interesting 1D ideal Einsteinian crystal based on the Boyer repulsive interaction.

We start with the two-plate Boyer setup. A point on each plate is described by $x_\alpha(x) = (\mathbf{x}, \delta_{\alpha,2}H)$, where $\alpha = 1$ and 2 identifies the plate, $\delta_{\alpha,2}$ is the Kronecker delta function, $x = (\mathbf{x}, x_0)$, x_0 is the temporal component, and $\mathbf{x} = (x_1, x_2)$ defines two lateral spatial coordinates. For the geometry we are considering, by decomposing the EM field into the transverse magnetic (TM) and the transverse electric (TE) waves [28] all components of the EM field can be expressed by the scalar fields $\Phi_{\rm TM} = B_\parallel$ and $\Phi_{\rm TE} = E_\parallel$, where $B_\parallel$ and $E_\parallel$ are the components of the magnetic and electric fields parallel to the surfaces of the plates. For the scalar field $\Phi_{\rm TM}$ Dirichlet (D) and Neumann (N) boundary conditions (BCs) are satisfied by the infinitely polarizable and infinitely permeable plates, respectively, while for the scalar field $\Phi_{\rm TE}$ an N BC and a D BC are satisfied by the infinitely polarizable and infinitely permeable plates, respectively [18]. Using the Matsubara formalism [13, 27] the partition function in the presence of two parallel plates can be written as

$$Z = \int \left[\mathcal{D}\Phi\right]_{\mathcal{C}} e^{-S[\Phi]/\hbar}, \tag{1}$$

where we ignored the inessential normalization w.r.t the partition function of the free space. Φ is a scalar field, subscript $\mathcal{C}$ denotes the constraint imposed by the plates on the scalar field and the model Euclidean action describing the field is assumed to be

$$S[\Phi] = \frac{1}{2}\int_0^\beta d\tau \int d^3x \left[\left(\frac{\partial\Phi}{\partial\tau}\right)^2 + (\nabla\Phi)^2\right]. \tag{2}$$

Here $\beta = \frac{1}{k_B T}$, with k_B the Boltzmann constant. As the scalar bosonic field satisfies the periodicity condition, $\Phi(x,\beta) = \Phi(x,0)$, one can expand it as $\Phi(x,\tau) = \sum_{n=-\infty}^{\infty}\Phi_n(x)e^{i\omega_n\tau}$ where $\omega_n = \frac{2\pi n k_B T}{\hbar}$ are the Matsubara frequencies. $\Phi(x,\tau)$ is real and must satisfy mixed boundary conditions, as explained above [18], i.e. for TM waves a D BC must be satisfied at the infinitely polarizable plate, while an N BC must be satisfied at the infinitely permeable plate. The Matsubara approach [13, 27] then yields the partition function for a pair of plates, where one has an N and the other one a D BC as (up to a multiplicative constant)

$$Z_{DN} = \int \prod_{n=-\infty}^{\infty} \mathcal{D}\Phi_n \delta(\Phi_n(X_1))\delta(\partial_N\Phi_n(X_2))e^{-S[\Phi]} \tag{3}$$

where ∂_N is the partial derivative in the normal direction to the surface. Integrating over Φ_n the logarithm of the partition function for the TM waves can be expressed as $\ln Z_{DN} = \sum_{n=-\infty}^{\infty}\ln\{det[\Gamma_n^{DN}]\}$ where

$$\Gamma_n^{DN} = \begin{pmatrix} G_n(x-y,0) & \partial_z' G_n(x-y,-H) \\ \partial_z G_n(x-y,H) & \partial_z\partial_z' G_n(x-y,0), \end{pmatrix} \tag{4}$$

with the free space Green's function $G_n(X_\alpha(x), Y_\sigma(y)) = \frac{e^{-\omega_n|X_\alpha(x)-Y_\sigma(y)|}}{4\pi|X_\alpha(x)-Y_\sigma(y)|}$. The prime is used for the derivative with respect to the second variable, i.e. y. A similar procedure can be applied for the TE waves to obtain the logarithm of the partition function, $\ln Z_{ND}$, with an N BC on the infinitely polarizable plate and a D BC on the infinitely permeable plate, and $\ln Z_{ND} = \ln Z_{DN}$. The normal Boyer force between the two plates can then be obtained from the free energy $\mathcal{F} = -k_B T[\ln Z_{ND} + \ln Z_{DN}]$ as $F = -\frac{\partial\mathcal{F}}{\partial H}$, with

$$\frac{F(T,H)}{A} = k_B T \sum_{n=-\infty}^{\infty}\int_0^\infty \frac{pdp}{\pi}\frac{\rho_n}{1+e^{2\rho_n H}}, \tag{5}$$

where

$$\rho_n = \sqrt{p^2 + \omega_n^2/c^2},$$

$p^2 = p_1^2 + p_2^2$, and p_1 and p_2 correspond to x_1 and x_2 coordinates in the Fourier space, respectively. The force at $T = 0$K can be calculated by replacing the Matsubara summation with a continuous integral as $\frac{F(T=0\text{K},H)}{A} = \frac{7}{8}\frac{\hbar c\pi^2}{240H^4} = -\frac{7}{8}F^C$. This expression is in complete agreement with the previous result of Boyer [16–18]. At finite temperature the force can be cast into an alternative form

$$\begin{aligned}\frac{F(T,H)}{A} &= \frac{3k_B T\zeta(3)}{16\pi H^3} + \frac{2k_B T}{\pi}\sum_{n=1}^{\infty}\int_0^\infty pdp\frac{\rho_n}{1+e^{2\rho_n H}} \\ &= k_B T\sum_{n=1}^{\infty}F_n(T,H),\end{aligned} \tag{6}$$

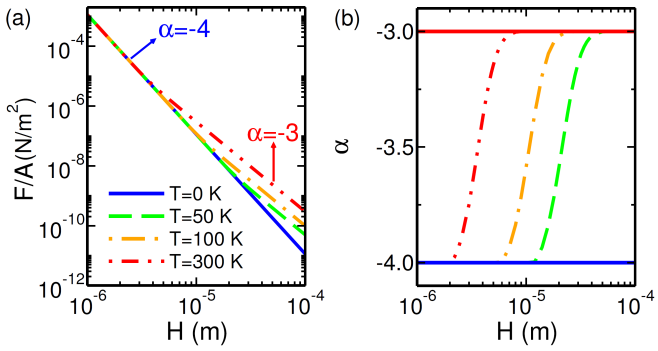

FIG. 2: (a) Boyer force per unit area, $F(T,H)/A$, as a function of the separation between two plates, H, for various values of temperature $T = 0 - 300$K (from bottom to top). α is the force exponent which is defined as $F/A \sim H^\alpha$. $\alpha = -4$ and -3 identify the quantum and classical regimes, respectively. (b) α as a function of H for various values of temperature as of panel (a). Here blue and red horizontal solid lines pertain to the quantum and classical regimes, respectively.

where the first term, $\frac{3k_BT\zeta(3)}{16\pi H^3}$, is the zero Matsubara frequency term which is the value of the force at large separations or high temperatures. Comparing this with the Casimir interaction force $F^C(T,H)$ between two ideally polarizable (metallic) sheets at finite temperature [4, 6, 13, 14], we note that

$$F_n(T,H) = -F_n^C(T,H) + 2F_n^C(T,2H), \tag{7}$$

so that in every regime the Boyer interactions for the asymmetric ideally permeable - ideally conductive system can be mapped onto a symmetric Casimir interaction for ideal conductors.

In Fig. 2a we plot the Boyer force per unit area as a function of H for various values of the temperature $T = 0 - 300$K. For separations smaller than the thermal length $\lambda_T = \hbar c/(2\pi k_B T) \sim 1.2\mu$m at room temperature ($T = 300$K), all curves collapse onto the zero temperature curve, revealing that the quantum fluctuations play the main role in the interaction, with the force scaling as H^α and $\alpha = -4$. For $H > 1.2\mu$m, as the temperature increases, the role of thermal fluctuations is gaining in importance and at large separations it is the thermal fluctuations that dominate the interaction with the force exponent $\alpha = -3$. To distinguish the quantum from the classical regimes, Fig. 2b shows the force exponent, α as a function of H. The transition between the quantum and the classical regimes is shifted to smaller separations for higher temperatures. For comparison, the attractive force between two ideal metallic sheets goes from $\alpha = -4$ to $\alpha = -3$ on increase of the separation [13, 14].

In the double Boyer setup composed of three flat parallel plates, one ideally permeable between two ideally polarizable ones, all immersed in vacuo at finite temperature T (see Fig. 1), the Matsubara approach [13, 27] or the transfer matrix formalism [14, 29, 30] both yield the free energy per unit area as

$$\frac{\mathcal{F}^s}{A} = k_B T \sum_{n=-\infty}^{\infty} \mathcal{F}_n^s(H_1, H_2), \tag{8}$$

where

$$\mathcal{F}_n^s(H_1,H_2) = \int_0^\infty \frac{pdp}{2\pi} \ln\big[1 + e_n(H_1,H_2)\big], \tag{9}$$

and

$$e_n(H_1,H_2) = e^{-2\rho_n H_1} + e^{-2\rho_n H_2} + e^{-2\rho_n (H_1+H_2)},$$

with H_1 and H_2 the separations between left and right hand conductors and the middle permeable plate, thus implying $H_1 + H_2 = 2H$ as shown in Fig. 1. The force f per unite area that acts on the middle permeable plate can be calculated as

$$\frac{f}{A} = -\frac{\partial}{\partial H_1}\left(\frac{\mathcal{F}^s}{A}\right) + \frac{\partial}{\partial H_2}\left(\frac{\mathcal{F}^s}{A}\right) = k_B T \sum_{n=-\infty}^{\infty} f_n(H_1,H_2), \tag{10}$$

where

$$f_n(H_1,H_2) = \int_0^\infty \frac{pdp}{\pi} \frac{\rho_n[e^{-2\rho_n H_1} - e^{-2\rho_n H_2}]}{1 + e_n(H_1,H_2)}.$$

The total force on the middle plate is thus a superposition of the two forces that act from the left and from the right conductors on the middle, ideally permeable plate. As these two forces are repulsive, it follows from the symmetry of the system that the *stable equilibrium* corresponds to $H_1 = H_2$, see Eq. (10). This is not at odds with the general theorem on the absence of stable equilibria with Casimir forces, since it hinges upon interactions only between objects within the same class of material [31], an assumption obviously violated for the Boyer setup.

When the permeable plate is displaced towards either of the conductor plates by ε, the restoring force that acts on it can be calculated as a function of ε by setting $H_1 = H + \varepsilon$ and $H_2 = H - \varepsilon$. The direction of the force is always toward the stable equilibrium location (see Fig. 1) and its magnitude can be obtained to the first order w.r.t. ε in the Hookian form, $f = -k\varepsilon$, with the spring constant $k = k(H,T)$ defined as

$$\frac{k(H,T)}{A} = k_B T \sum_{n=-\infty}^{\infty} k_n(H,T), \tag{11}$$

where

$$k_n(H,T) = \int_0^\infty \frac{pdp}{\pi} \frac{4\rho_n^2 e^{-2\rho_n H}}{[1 + e^{-2\rho_n H}]^2}.$$

At low temperatures or small separations (quantum limit) the spring constant per unit area is $\frac{k(H,T\to 0)}{A} \to \frac{7\hbar c\pi^2}{240H^5}$, while at high temperatures or large separations (classical limit) $\frac{k(H,T\to\infty)}{A} \to \frac{9\zeta(3)k_BT}{8\pi H^4}$. In Fig. 3a we plot the magnitude of the normalized force, $|f|/k(H, T \to 0)$, as a function of ε, for various values of $H = 10^{-7} - 10^{-4}$m (from top to bottom). As is evident from the plot, the Hookian limit is valid within the range $|\varepsilon| < H/10$. In Fig. 3b the magnitude of the normalized Casimir force has been plotted as a function of ε at constant $H = 10^{-4}$m for $T = 0 - 300$K (from bottom to top). By increasing the temperature the spring constant also increases with the range of validity of the Hookian region remaining unchanged.

Fig. 3c presents the spring constant, $k(H,T)$, per unit area as a function of H for various values of temperature $T = 0 - 300$K (from bottom to top). Obviously at low temperatures or small separations the spring constant per unit area scales as H^{-5}, while at high temperature or large separations it scales as H^{-4}. Fig. 3d shows $|f|/A$ at $H = 10^{-4}$m as a function of $H_2 = H - \varepsilon$ for various values of temperature $T = 0 - 300$K (from bottom to top). For small values of H_2 the contribution of quantum fluctuations to the interaction dominates over that of the classical thermal fluctuations. Indeed at sufficiently small H_2 the force per unit area is $f/A = \frac{7}{8}\frac{\hbar c\pi^2}{240(H-\varepsilon)^4}$.

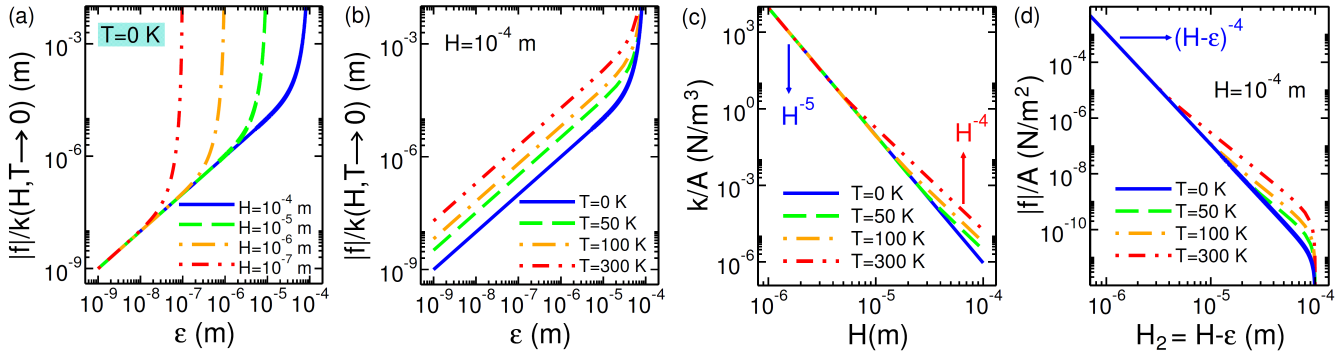

FIG. 3: (a) The magnitude of the normalized Boyer force, $|f|/k(H, T \to 0)$, as a function of the displacement of the middle ideally permeable plate from its equilibrium position, ε, for various values of the separation between equilibrium position of the permeable plate and each conductor, $H = 10^{-7} - 10^{-4}$m (from top to bottom). Here $k(H, T \to 0)$ is the spring constant of the Boyer interaction at zero temperature. (b) $|f|/k(H, T \to 0)$ at constant $H = 10^{-4}$m has been plotted as a function of ε for various values of temperature $T = 0 - 300$K (from bottom to top). (c) Spring constant per unit area, k/A, as a function of H for various values of temperature as of panel (b). (d) The magnitude of the force per unit area $|f|/A$, at constant $H = 10^{-4}$m as a function of the separation between permeable plate and right conductor, $H_2 = H - \varepsilon$, for various values of T as of panels (b) and (c).

If the middle permeable plate is free to move, the eigenfrequencies of such Boyer oscillator at a finite temperature are then given by $\omega^2(H,T) = \frac{k(H,T)}{m}$ where m is the mass of the plate. Assuming it has a thickness d and a cross section area A, using $m = \varrho dA$, where ϱ is the mass density, the eigenfrequency in the two temperature limits becomes

$$\omega^2(H, T \to 0) = \frac{7\hbar c\pi^2}{240H^5\varrho d}, \tag{12}$$

and

$$\omega^2(H, T \to \infty) = \frac{9\zeta(3)k_BT}{8\pi H^4\varrho d}. \tag{13}$$

Interestingly, ω is not a function of the cross section area A. Given the mass density of YIG as $\varrho = 5.172\text{gr/cm}^3$ the magnitude of the frequency for $d = 12.4$nm is $\omega(H, T \to 0) = 1.9$kHz, and 0.6MHz at $H = 1\mu$m and $H = 0.1\mu$m, respectively, and $\omega(H, T \to 0) = 0.6$GHz when $d = 1.24$nm and $H = 10$nm. In the classical regime, by choosing $H = 10\mu$m and $T = 300$K, the eigenfrequencies are obtained as $\omega(H, T = 300K) = 152.1$Hz, 48.1Hz and 15.2Hz for $d = 1.24$nm, $d = 12.4$nm and $d = 124$nm, respectively.

Finally, we examine the elastic modulus of the system at constant temperature, K, defined as the inverse of the compressibility at constant temperature, $-\frac{1}{V}\left(\frac{\partial V}{\partial P}\right)_T$ where V is the volume and P is the pressure of the system. The elastic modulus for the double Boyer setup, Fig. 1, for $H_1 = H_2$ then becomes

$$K(H,T) = \frac{H}{A}\left(\frac{\partial^2\mathcal{F}^s(H,T)}{\partial H^2}\right) = \frac{H}{2A}k(H,T). \tag{14}$$

At very low temperatures or small separations $K(H, T \to 0) \to \frac{7\hbar c\pi^2}{480H^4}$ while at high temperature or large separation limits $K(H, T \to \infty) \to \frac{9\zeta(3)k_BT}{16\pi H^3}$. The magnitude of the elastic modulus for $T = 0$K at $H = 1$nm is $K = 4.55$GPa which is about twice that of water at $T = 293$K.

Interestingly, the bulk modulus for a multi-layer Boyer system (B_N) composed of $N + 1$ flat ideal conductors and N flat ideal permeable plates, depicted in Fig. 4, so that each permeable plate is located between two adjacent ideal conductors, with the separation between each plate with its neighboring plates being H, is the same as for the system composed of one permeable plate between two conductors. This is due to the fact that the conducting plates ideally screen the field. Allowing for the free

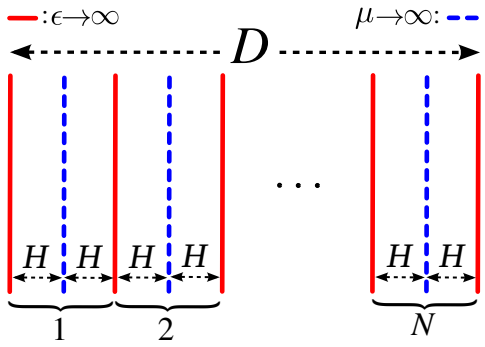

FIG. 4: Schematic geometrical picture of the multi-layers system composed of $N + 1$ flat ideal conductors ($\epsilon \to \infty$) and N flat ideal permeable ($\mu \to \infty$) plates. Each permeable plate is located between two conductors, and each conductor is located between two permeable plates except the first and the last conductors. The distance between each plate with its neighboring plates is H, and the full width of the Boyer oscillator array is $D = 2NH$ in the limit of $H \gg d$, where d is the thickness of each ideal plate.

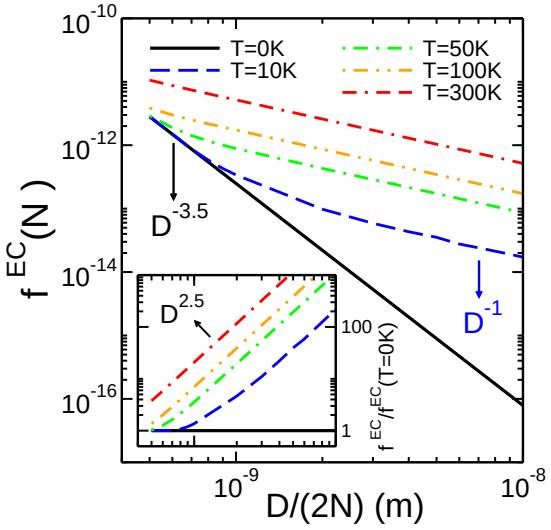

FIG. 5: Fluctuation force, $f^{\rm EC}$, as a function of the width of each cell, $\frac{D}{2N}$, in the oscillators array, for various values of the temperature of the system, $T = 0 - 300$K (from bottom to top). Inset shows the normalized fluctuation force, $f^{\rm EC}/f^{\rm EC}(T = 0{\rm K})$, as a function of $\frac{D}{2N}$.

displacement of the ideally permeable plates, we then get a Boyer oscillator array, which can in fact be described as an ideal *Einsteinian crystal* since the displacements of the different oscillators are not coupled.

The free energy of such an Einsteinian crystal , $\mathcal{F}^{\rm EC}$, can then be calculated as

$$\mathcal{F}^{\rm EC}(D,T) = -Nk_BT\log\mathcal{Z}\left(\frac{D}{2N},T\right) = \\ = \frac{N}{2}\hbar\omega\left(\frac{D}{2N},T\right) + Nk_BT\log\left(1-e^{-\beta\hbar\omega(\frac{D}{2N},T)}\right), \quad (15)$$

where $H = \frac{D}{2N}$ (in the limit of $H \gg d$) and D is the total width of the Boyer oscillator array, while $\mathcal{Z}(\frac{D}{2N},T)$ is the partition function of a single Boyer harmonic oscillator. This gives us another fluctuation force acting between the boundaries of the array, dependent on the original Boyer repulsion within a single oscillator in the array. In the different temperature limits we obtain from Eqs. (12) and (13) to the lowest order

$$\mathcal{F}^{\rm EC}(D,T\to 0) = \frac{N^{7/2}}{2}\sqrt{\frac{7\ 2^5\ \hbar^3c\pi^2}{240\ D^5\varrho d}}, \quad (16)$$

and

$$\mathcal{F}^{\rm EC}(D,T\to\infty) = \frac{Nk_BT}{2}\log\left(\frac{18N^4}{\pi\ D^4\varrho d}\right). \quad (17)$$

We see that in both limits the total free energy corresponds to a repulsive interaction and is not extensive in the number of oscillators, while the dependence on the width of the Boyer oscillator array has a different form than the H dependence of the Boyer interaction for each of the oscillators. Obviously for large temperatures the fluctuation interaction between the boundaries of a Boyer array is an anomalously long-ranged function of the extension of the array, decaying algebraically as D^{-1}. The fluctuation force between the boundaries of the Boyer oscillator array, $f^{\rm EC} = -\frac{\partial\mathcal{F}^{\rm EC}}{\partial D}$, can be derived as

$$f^{\rm EC}(D,T\to 0) = 5\left(\frac{N}{D}\right)^{\frac{7}{2}}\sqrt{\frac{7\hbar^3c\pi^2}{120\varrho d}}, \quad (18)$$

and

$$f^{\rm EC}(D,T\to\infty) = \frac{2Nk_BT}{D}, \quad (19)$$

respectively. In Fig. 5 the fluctuation force, $f^{\rm EC}$, has been plotted as a function of the width of each cell, $\frac{D}{2N}$, in the oscillator array, for various values of the temperature of the system, $T = 0 - 300$K (from bottom to top), with $d = 1.24$Å and $\varrho = 5.127{\rm gr/cm}^3$. As is clear, for low temperatures and small distances limits the force scales as $D^{-\frac{7}{2}}$, while for large separations or high temperatures it scales as D^{-1}. To show these scaling behaviors more clearly the normalized fluctuation force, $f^{\rm EC}/f^{\rm EC}(T = 0{\rm K})$, has been plotted as a function of $\frac{D}{2N}$. The slope of the curve for the normalized force at $T = 300$K is equal to $+2.5$ for the whole range of the separations which reveals the high temperature limit. As the temperature decreases the slope of the normalized force curve decreases at small separations due to the quantum fluctuations.

Boyer interaction between a flat ideal conductor and a flat ideally permeable plate is repulsive and depends strongly on the temperature of the system. At small separations or very low temperatures, only quantum fluctuations play a role in the interaction (quantum regime), while at intermediate separations or moderate temperatures (transient regime) both quantum and thermal fluctuations are important. At large separations or high temperatures (classical limit) the interaction is governed mainly by the contribution of the classical thermal fluctuations. For a Boyer system composed of three flat parallel plates, one permeable plate between two conductors, all immersed in vacuo at a finite temperature, the system possesses a stable equilibrium when the middle permeable plate is located exactly in the middle of the cavity. For small values of displacement from this stable equilibrium the force is Hookian and the corresponding spring constant is a function of the separation between the two bounding conductors and the temperature. Harmonic vibrations around this stable equilibrium value define a Boyer oscillator with temperature dependent eigenfrequencies. A linear array of such oscillator behaves as an ideal Einsteinian crystal and the confined fluctuations of ideally permeable plates around their equilibrium positions induces a fluctuation interaction between its boundaries. While being related to the Boyer interaction, producing a restoring force within a

single oscillator, the fluctuation interaction between the boundaries of the Boyer array has a very different separation dependence in the limit of small and large temperatures.

Acknowledgments

J.S. acknowledges support from the Academy of Finland through its Centers of Excellence Program (2012-2017) under Project No. 915804. R.P. acknowledges support from the ARRS through Grant No. P1-0055.

[1] H. B. G. Casimir, Proc. K. Ned. Akad. Wet. **51**, 793 (1948).
[2] P. W. Milonni, The quantum vacuum: *an introduction to quantum electrodynamics* (Academic Press, 1994).
[3] E. M. Lifshitz, Sov. Phys. JETP **2**, 73 (1956).
[4] V. A. Parsegian, *Van der Waals Forces* (Cambridge University Press, Cambridge 2005).
[5] R. French *et al.*, Rev. Mod. Phys. **82**, 1887 (2010).
[6] M. Bordag, G. L. Klimchitskaya, and U. Mohideen, *Advances in the Casimir effect* (Oxford University Press, 2009).
[7] M. Kardar and R. Golestanian, Rev. Mod. Phys. **71**, 1233 (1999).
[8] J. Sarabadani and M.F. Miri, Phys. Rev. A **74**, 023801 (2006).
[9] J. Sarabadani and M.F. Miri, Phys. Rev. A **75**, 055802 (2007).
[10] F. Kheirandish, M. Soltani and J. Sarabadani, Phys. Rev. A **81**, 052110 (2010).
[11] M. Soltani, J. Sarabadani, F. Kheirandisg and H. Rabbani, Phys. Rev. A **82**, 042512 (2010).
[12] F. Kheirandish, M. Soltani and J. Sarabadani, Ann. Phys. (NY) **326**, 657 (2011).
[13] J. Sarabadani and M.F. Miri, Phys. Rev. A **84**, 032503 (2011).
[14] J. Sarabadani, A. Naji, R. Asgari and R. Podgornik, Phys. Rev. B **84**, 155407 (2011).
[15] J. Sarabadani, M. Soltani, P. Zakeri and S. A. Jafari, Phys. Rev. A **86**, 022507 (2012).
[16] T. H. Boyer, Phys. Rev. A **9**, 2078 (1974).
[17] V. Hushwater, Am. J. Phys **65**, 381 (1997).
[18] B. Kiani and J. Sarabadani, Phys. Rev. A **86**, 022516 (2012).
[19] L. M. Woods, D. A. R. Dalvit, A. Tkatchenko, P. Rodriguez-Lopez, A. W. Rodriguez and R. Podgornik, Cond-mat arXiv:1509.03338 (2015).
[20] A. A. Feiler, L. Bergstrom and M. W. Rutland, Langmuir **24**, 2274 (2008).
[21] S. Lee and W. M. Sigmund, J. Colloid Interface Sci. **243**, 365 (2001).
[22] A. Milling, P. Mulvaney and I. Larson, J. Colloid Interface Sci. **180**, 460 (1996).
[23] J. N. Munday, F. Capasso and V. A. Parsegian, Nature **457**, 170 (2009).
[24] C.-G. Shao, D.-L. Zheng and J. Luo, Phys. Rev. A **74**, 012103 (2006).
[25] E. Buks and M. L. Roukes, Nature (London) **419**, 119 (2002).
[26] M. Nasiri and M.F. Miri, Phys. Rev. E **85**, 041102 (2012).
[27] J. I. Kapusta, *Finite-Temperature Field Theory* (Cambridge University Press, 1989).
[28] J. D. Jackson, *Classical Electrodynamics* (Wiley, New York, 1999).
[29] R. Podgornik, P. L. Hansen and V. A. Parsegian, J. Chem. Phys. **119**, 1070 (2003).
[30] R. Podgornik, R. H. French and V. A. Parsegian, J. Chem. Phys. **124**, 044709 (2006).
[31] S. J. Rahi, M. Kardar and T. Emig, Phys. Rev. Lett. **105**, 070404 (2010).